Spatial-temporal variations in evapotranspiration along the East Coast of North America: Contribution of land use, climate, and atmospheric CO_2

Qichun Yang, Hanqin Tian*, Xia Li, Bo Tao, Wei Ren, Guangsheng Chen, Chaoqun Lu, Jia Yang, Shufen Pan, Kamaljit Banger, Bowen Zhang

International Center for Climate and Global Change Research and School of Forestry and Wildlife Sciences, Auburn University, Auburn, AL, 36849, USA

*Corresponding author. Tel: +1 334 844 1059; Fax: +1 334 844 1084. Email: tianhan@auburn.edu

Mar, 2014

To be submitted to Ecohydrology

ABSTRACT

The east coast region of North America (NAECoS) has experienced significant land use and climate changes since the past century. In this study, the Dynamic Land Ecosystem Model (DLEM) 2.0 with time-series input data of land use, climate, and atmospheric CO_2 was used to examine how these driving forces affected the spatial and temporal variability of evapotranspiration (ET) in this region during 1901-2008. Results indicated that the average ET in the NAECoS was 648.3±38.6mm/year and a significant increasing trend was found from 1901 to 2008. Factorial model simulations indicated that climate change was the primary factor (76.3%) for controlling the interannual variability of ET, while land use change effects were significant on decadal and century scales. Although land use change only explained 15.9% of the ET temporal variability, afforestation significantly increased ET by 12.8 mm/ year. Elevated atmospheric CO_2 reduced ET at a rate of 0.84 mm/year and its impact should be further investigated with future CO_2 concentration increases. Climate change determined the spatial pattern of ET variability over the study area, whereas land use change demonstrated substantial impacts on ET at watershed scales.

Key words: The North America East Coast (NAECoS), Land use change, Climate change, Atmospheric CO_2 Elevation, Evapotranspiration (ET), Dynamic Land Ecosystem Model (DLEM).

INTRODUCTION

Investigation of land surface ET and the underlying mechanisms affecting its variability is the key to understandings of a series of hydrological, ecological and economic issues such as runoff, drought and agricultural production (Jung *et al.*, 2010; Liu *et al.*, 2012). Land surface ET is controlled by a variety of factors including solar radiation, precipitation, wind speed, temperature, vegetation structure, and soil properties (Bosch and Hewlett, 1982; Dunn and Mackay, 1995; Sun *et al.*, 2005; Tomer and Schilling, 2009). Influence of land conversions on ET mainly lies in changes of hydrological properties of vegetation and soil layers which alter the energy and water exchanges between land surface and the atmosphere (Schilling and Libra, 2003; Zhang and Schilling, 2006; Bormann *et al.*, 2007). Land management practices such as crop cultivation, irrigation, and tillage also influence ET through changing plant phenology, soil water content, and soil structure (Liu *et al.*, 2008; Tian *et al.*, 2011a). Climate factors like solar radiation, temperature and precipitation control energy availability, water vapor demand and soil moisture supply for ET. Interactions of climate factors affect the spatial variations of ET over large areas. In addition, increasing atmospheric CO_2 is another factor that may induce changes in ET (Jarvis and Morrison 1981). In elevated CO_2 treatments, plants tend to increase stomatal resistance. Negative relationships between CO_2 concentration and ET have been observed in chamber experiments for different plant species (Baker *et al.*, 1990; Medlyn *et al.*, 2001; Shams *et al.*, 2012).

Although great efforts have been devoted to investigate ET responses to changing land use and climate conditions, knowledge gaps still exist in understandingregional ET dynamics in the context of global changes. First, contributions of different environmental factors and their interactions need to be further addressed to uncover the underlying mechanisms that control

regional ET. Current knowledge about land use change effects on ET is mainly derived from paired catchment experiments which concluded that afforestation generally increase ET (Bosch and Hewlett, 1982). However, some other studies argued that tree species and climate conditions should be considered in interpreting the results of watershed experiments (Jones and Post, 2004). In addition to land use change impacts, influence of changing climate on ET should also be further explored. Previous studies have concluded that global warming would enhance ET (Law *et al.*, 2002; Goyal, 2004), while some others emphasized the impacts of precipitation and indicated that changing precipitation plays the dominant role in regional ET variability over long time periods (Nagler *et al.*, 2007; Jung *et al.*, 2010). In addition, although plant transpiration was found to decline with increasing atmospheric CO_2 due to reduction in stomatal conductance, this effect can be mitigated by the increasing LAI under high CO_2 concentrations (Kergoat *et al.*, 2002). Impacts of these two counteracting mechanisms on ET over large areas need to be investigated as atmospheric CO_2 is project to increase in the future (Lindroth, 1996). To reduce uncertainties in estimation of regional ET, it is necessary to systematically analyze ET dynamics by taking the impacts of different environmental factors into consideration.

Since the beginning of the 20th century, large area of cropland was abandoned and afforested in the North America east coast region (NAECoS) (Ramankutty and Foley, 1999). Meanwhile, this area also underwent significant climate changes (Walsh *et al.*, 2013). To improve our understanding of multiple environmental factors' impacts on regional ET, a fully distributed and process-based ecosystem model – the Dynamic Land Ecosystem Model (DLEM 2.0) – was applied to reconstruct the historical ET from 1901 to 2008 over this area. By developing spatially and temporally-explicit input data and performing factorial model simulations, the long-term ET variability in response to land use change and climate change as well as atmospheric CO_2

elevation was analyzed. Objectives of this study include: (1) reconstructing the historical ET of the NAECoS during 1901-2008; (2) quantifying the relative contributions of different environmental factors on ET variability; (3) investigating interactive effects of different environmental factors on ET variability from temporal and spatial perspectives.

STUDY AREA

[Figure 1]

The NAECoS extends from Nova Scotia, Canada to southern Florida, U.S. and covers most of the watersheds that drain into the Atlantic Ocean in the U.S. and part of Canada (Figure 1). The total area of this region is 870,000km^2 and the total population is about 85 million (Waisanen and Bliss, 2002). This drainage area consists of a variety of ecosystems types due to the significant climate variability from north to south (from 23° N to 48° N). As a densely populated region, the NAECoS underwent dramatic land use changes since the past century. Since 1901, large areas of cropland have been abandoned and replaced by forests. Meanwhile, urban area increased by about 3 million hectares between 1972 and 2000 (Drummond and Loveland, 2010). Climate change has demonstrated varied patterns in the whole area. According to Walsh et al. (2013), temperature increased in northeastern states but decreased in parts the southeastern states of the U.S. during the 20th century; precipitation increased has in Northeast U.S. but decreased in Southeast U.S. since 1901.

RESEARCH METHOD

ET Simulation in DLEM 2.0

[Figure 2]

In this study the DLEM 2.0 was applied to simulate ET in the NAECoS. DLEM 2.0 is a grid cell-based ecosystem model which is able to simulate major biogeochemical cycles, water cycle, and vegetation dynamics in terrestrial ecosystems (Figure 2). Detailed descriptions of DLEM and its applications can be found from our recent publications (Tian *et al.*, 2009, 2010, 2011a, 2011b, 2012b; Ren *et al.*, 2011; Chen *et al.*, 2012; Lu and Tian, 2012; Liu *et al.*, 2013; Tao *et al.*, 2013).

Processes related to ET simulation in DLEM 2.0 are briefly introduced here. Detailed descriptions of how water cycling is simulated in DLEM 2.0 can be found in Liu *et al*. (2013). Plant transpiration in DLEM 2.0 is calculated with the Penman-Monteith equation (Wigmosta *et al.*, 1994). In the model the canopy conductance and resistance are up-scaled from the two-leaf model (Landsberg, 1986).

$$E_t = \frac{\Delta R_n + \rho c_P (e_s - e)(g_c)_j}{\lambda_v(\Delta + \gamma(1 + (g_c)_j/(g_s)_j))} \quad (1)$$

$$(g_c)_j = \frac{LAI_j^{sun}}{(r_s^{sun})_j} + \frac{LAI_j^{sha}}{(r_s^{sha})_j} \quad (1.1)$$

$$(r_c)_j = 1/(g_c)_j \quad (1.2)$$

where E_t is the water transpiration rate ($m^3/s/m^2$); Δ is the slope of saturated vapor pressure-temperature curve (Pa/k); R_n is the net radiation flux density (W/m^2); ρ is the air density (kg/m^3); λv is the latent heat for water vaporization (J/g); γ is the psychrometric constant; j is the jth plant functional type (PFT); g_c and g_s are the canopy conductance and stomatal conductance, respectively (m/s); r_s^{sun} and r_s^{sha} are the stomatal resistance of sunlit leaves and shaded leaves

(s/m), and LAI_j^{sun} and LAI_j^{sha} are leaf area index for sunlit leaves and shaded leaves, respectively.

Stomatal conductance in the model is calculated with methods suggested by Hijmans *et al.*, (2005), Jarvis and Morison (1981), Running and Coughlan (1988) and Chen *et al.*(2005).

$$g_s = \max(g_{max} r_{corr} b f(ppdf) f(T_{min}) f(vpd) f(CO_2), g_{min}) \tag{2}$$

$$r_{corr} = \left(\frac{T_{day}+273.15}{293.15}\right)^{1.75} \times \left(\frac{101300}{p}\right) \tag{2.1}$$

$$f(ppdf) = \frac{ppdf}{75+ppdf} \tag{2.2}$$

$$b_i = \begin{cases} 1 & \psi_i > \psi_{open} \\ \frac{\psi_{open}-\psi}{\psi_{open}-\psi_{close}} & \psi_{close} \le \psi_i \le \psi_{open} \\ 0 & \psi_i < \psi_{close} \end{cases} \tag{2.3}$$

$$b = \sum_{i=1}^{10}\left(root_i \frac{\theta_{sat,i}-\theta_{ice,i}}{\theta_{sat,i}} b_i\right) \tag{2.4}$$

$$f(T_{min}) = \begin{cases} 1 & T_{min} > 0°C \\ 1 + 0.125T_{min} & -8°C \le T_{min} \le 0°C \\ 0 & T_{min} < -8°C \end{cases} \tag{2.5}$$

$$f(vpd) = \begin{cases} 1 & vpd < vpd_{open} \\ \frac{vpd_{close}-vpd}{vpd_{close}-vpd_{open}} & vpd_{open} \le vpd \le vpd_{close} \\ 0 & vpd > vpd_{close} \end{cases} \tag{2.6}$$

$$f(CO_2) = -0.001CO_2 + 1.35 \tag{2.7}$$

where g_s is the stomatal conductance; r_{corr} is the correction factor of temperature and air pressure on conductance; b is the soil moisture factor; *ppdf* is the photosynthetic photo flux density (umol/ m^2 s); T_{min} is the daily minimum T (°C); *vpd* is the vapor pressure deficit (pa); CO_2 is the atmospheric CO_2 concentration (ppm); g_{max} and g_{min} is the maximum and minimum stomatal

conductance for water vapor, respectively (m/s). p is the air pressure (pa); $\theta_{sat,i}$ is the ith soil layer saturated volumetric water content (mm H_2O/ m^2) ; $\theta_{ice,i}$ is the volumetric ice content of the ith soil layer (mm H_2O/ m^2) ; ψ is the water potential (mm H_2O) ; ψ_{open} and ψ_{close} are the water potential under which the stomata fully open and close, respectively (mm H_2O) ; vpd_{close} and vpd_{open} are the vapor pressure deficit when leaf stomata is fully closed and open, respectively (Pa).

For simulation of soil moisture dynamics in different soil layers the water movement scheme developed by Oleson et al., (2008) was adopted in DLEM 2.0. For irrigated cropland, if the estimated transpiration is larger than available soil water, then water deficiency is assumed to be replenished by irrigation. The equations for bare-ground evaporation simulation used by Food and Agriculture Organization (FAO) was adopted and improved in DLEM 2.0 (Allen et al., 1998). Improvements were made to consider influence of vegetation canopy on net radiation and aerodynamic resistance. First, shortwave radiation through canopy is used as the energy source in Penman-Monteith equation to estimate the potential soil evaporation (*PSE*). Then, the *PSE* is adjusted by leaf area according to Belmans *et al.* (1983):

$$EVAP = pet_{PM} e^{-0.6LAI} \tag{3}$$

where *EVAP* is the soil evaporation; pet_{PM} is the potential ET estimated with the Penman-Monteith equation, and *LAI* is the average LAI over the land area in each grid.

Input data development

[Table I]

A variety of datasets with a spatial resolution of 5 × 5 arc-minutes (around 9.2 × 9.2 km^2 at the equator) were developed for our study area to drive the model (Table I). Total land area in each grid was calculated from the GLC2000 North America grid dataset (Latifovic *et al.*, 2004). The distributions of contemporary PFTs were integrated from multiple data sources such as the GLC2000, global potential vegetation map from Ramankutty and Foley (1999), and the Global Lakes and Wetlands Database (Lehner and Döll, 2004). Impervious surface data were derived from the History Database of the Global Environment (HYDE) with the version of HYDE2005 (Klein Goldewijk and Ramankutty, 2004). Total vegetated area in each grid was obtained by subtracting non-vegetation covers (i.e. impervious surfaces, lakes, streams, glaciers, and oceans) from the total grid area. For cropland, a cropping system dataset was produced by combining the information from the U.S. Census of Agriculture and the global cropland distribution data from Monfreda *et al.*(2008). The irrigation data used in DLEM 2.0 was developed based on the International Water Management Institute (IWMI)'s Total Area Available for Irrigation (TAAI) database (Thenkabail et al., 2008). The historical daily climate data was derived from the CRU TS 2.1 dataset and the North America Regional Reanalysis (NARR) dataset (Mitchell and Jones, 2005; Mesinger *et al.*, 2006). The monthly CRU was downscaled with daily patterns of the NARR data to make seamless combinations of these two datasets. For relative humidity and solar radiation dataset, NARR data (1981-2008) are used to reconstruct data in the historical periods (1901-2008) by assuming that these two datasets do not have long-term trends. The final products contain the historical information of monthly anomalies in precipitation and temperature which were from CRU and the daily and spatial patterns from the NARR data. Detailed description of how climate data were processed can be found in Liu et al.(2013).The daily and spatial atmospheric CO_2 data is provided by the Oak Ridge National Lab Multi-scale

Synthesis and Terrestrial Model Intercomparison Project (Wei *et al.*, 2013). Detailed descriptions of how these input data were developed and organized to drive DLEM 2.0 can be found in Liu *et al.* (2013).

Model simulation design

[Table II]

The DLEM 2.0 simulation includes three steps: the equilibrium run, the spin-up run, and the transient run (Tian *et al.*, 2012a). In the equilibrium run, it is assumed that natural ecosystem should reach an equilibrium state at stable climate conditions. Standard adopted for this equilibrium state is that the net carbon exchange for 20 consecutive years is less than 0.5g C/m^2, the net water pool change is less than 0.5 mm and the net nitrogen change is less than 0.5g N/m^2. At this step, the model is driven by average climate condition from 1901 to 1930 and land use data in 1900. After that three thirty-year spin-up runs were conducted to reduce the biases resulted from climate data in the simulations (Thornton and Rosenbloom, 2005). In the transient run, annual land use data and daily climate data from 1901 to 2008 were used to drive the model to produce transient simulation of ecosystem dynamics.

In this study, five simulations were conducted to quantify relative contributions of different environmental factors to ET variability (Table II). The major environmental factors considered in this study include land use change, climate change and atmospheric CO_2 increase. The 'Control' simulation was to quantify biased estimates caused by model configuration (Huntzinger *et al.*, 2012). For the 'Control' simulation, the averaged climate data and atmospheric CO_2 data from 1901 to 1930 and the land use data of 1901 were used as input for the simulation during 1901-2008. Results of this simulation were used as the baseline for the other four simulations. For the 'Climate only' simulation, transient climate data for the whole study period were used but

atmospheric CO_2 data and land use data were held constant (average atmospheric CO_2 data from 1901 to 1930 and land use data in 1901). For the 'CO_2 only' simulation, transient CO_2 data for the whole study period were used while the other input data including climate, land use data were held constant (Climate data from 1901 to 1930 and land use data in 1901). Similarly, in the 'Land use change only' simulation, dynamic land use data were used to drive the model while climate data and CO_2 were kept unchanged. For the 'All' simulation, effects of climate change, land use change and atmospheric CO_2 elevation on ET were considered by feeding the model with the reconstructed temporally and spatially-explicit input data for the period from 1901 to 2008.

Model Calibration

Throughout the development of DLEM, a plethora of field observations have been used to calibrate model parameters for simulations of carbon and water fluxes (Chen *et al*., 2012; Lu & Tian, 2012; Ren *et al*., 2011; Tao *et al*., 2013; Tian *et al*., 2010, 2012; Tian, Lu, *et al*., 2011; Xu *et al*., 2010). These data, including primary production, plant biomass, soil carbon storage, vegetation and soil nitrogen content, greenhouse gas emissions, were used for parameter calibration. In this study, parameters related to ET processes were recalibrated since the model structure and equations related to ET simulation in DLEM 2.0 were improved compared with the previous versions. Observed ET data derived from AmeriFlux sites were used for calibrating parameters for different PFTs.

Statistical Analysis

To demonstrate the temporal and spatial variability of climate factors and evapotranspiration, the Mann-Kendall test was used to analyze the input climate data and model simulations. Besides

time series analysis of average temperature, precipitation and ET over the whole region, trends and changing rates of input climate factors and ET were also calculated for each grid cell to demonstrate the spatial variations of these variables. Changing rate was calculated with the Sen's Slope test. Confidence level was set to 95% to detect weather trends existed in long-term time series.

RESULTS

Model performance evaluation

[Figure 3]

[Figure 4]

[Figure 5]

Daily ET simulations were plotted against daily ET observation at one AmeriFlux site located in the NAECoS (Figure 3). The Loblolly pine forest site in North Carolina was selected for the ET comparisons in 2005 and 2006. Figure 3 showed that ET estimation by DLEM 2.0 has similar seasonal patterns with observation data, with high ET in summer and low ET in winter. The simulated ET was comparable to the observational data in both magnitude and changing trends. For example, average simulated ET was 3.12 mm/day, while observation was 2.90 mm/day. Significant relationships between simulation and observation were also found ($p<0.001$).

In addition, we also compared the simulated annual ET with field observations at 21 Ameriflux sites which cover all the plant functional types in the NAECoS. Figure 4 showed that DLEM 2.0 ET simulations are comparable with observation data at most sites in average ET and standard deviations. This suggested that DLEM 2.0 is capable of providing reasonable representation of ET over different plant functional types. There were larger discrepancies

between simulated and observed ET for some sites. For example, at the Brookings site (US-Bkg), ET was underestimated by 25%; at the Howland Forest Main site (US-Ho1), ET was overestimated by 50%. One possible cause for the mismatch is due to the difference in climate data. The observed climate data at these two sites is greatly different from the regional climate data used by DLEM 2.0.

Finally, to evaluate DLEM 2.0 performance at regional scale, the simulated ET was compared to MODIS ET products (Mu *et al.*, 2011) for the period 2000-2008. The remotely sensed land cover information and other environmental factors were integrated in the algorithms for estimating ET in MODIS ET products. The comparisons indicated that DLEM 2.0 simulated ET agreed well with the MODIS dataset in terms of spatial distribution and magnitude (Figure 5). The DLEM 2.0 simulated average ET (ET from surface water and urban area was excluded to make it comparable with MODIS dataset) was 602 mm during 2000-2010 in the NAECoS , which was very close to the MODIS estimation (619 mm). As to the spatial distribution of ET in the study area, DLEM 2.0 and MODIS data reflected similar patterns which decreased along the latitudinal gradient from the southern Florida to Nova Scotia. Discrepancies existed in some areas. For example, DLEM-simulated ET in the northeastern NAECoS was lower than the MODIS ET, while DLEM 2.0 simulation was a little higher than MODIS data for croplands in the coastal plains of the southern NAECoS. The different land use data between DLEM 2.0 and MODIS could be one of the reasons for the inconsistency. However, the agreement of the two ET estimations based on different mechanisms demonstrated that DLEM 2.0 is capable of providing reasonable ET estimation in the NAECoS.

Environmental changes in the NAECoS during 1901-2008

[Figure 6]

Land use in the study area has changed substantially since 1901 (Figure 6). Due to the widespread abandonment of agricultural land, cropland has decreased by about 48% during 1901-2005. Forest area increased by about 12% from 1901 to 2000, but decreased slightly thereafter, mainly because of forest clearance for urban sprawl. The area of impervious surface had a dramatic increase of more than 250% as a result of urbanization from 1901 to 2010. Cropland abandonment mainly occurred in the central and southern NAECoS. Cropland area increased for some states, such as South Carolina, North Carolina, Georgia, and southern Florida.

[Figure 7]

[Figure 8]

[Table III]

In the past 108 years, the NAECoS has experienced dramatic climate changes. Average annual precipitation was 1064.2±164.3 mm/year (95% confidence interval) during 1901-2008. Interannual variability of precipitation tended to increase with time, indicating more frequent extreme weather events in recent decades. For example, during 1901-1978, standard deviation (STD) of annual precipitation was 75 mm/year, while for the period between 1979 and 2008, the STD increased to 98 mm/year. Seasonal analysis showed that rainfall in November has increased significantly, but with no statistically significant trends for other months (Table III). Spatial distribution of precipitation variability demonstrated significant heterogeneity (Figure 7A). The northern and southern NAECoS showed an opposite trend, with an increasing tendency in the north and a decreasing tendency in the south.

Annual mean temperature was 11.7±1.2°C (95% confidence interval) during 1901-2008. Average temperature demonstrated a significant increasing trend with a rate of 0.0079 °C/year

during 1901-2008 ($p < 0.01$) (Figure 8). Seasonality analysis showed that monthly maximum temperature in February, April, and August has increased significantly. Monthly mean temperature exhibited more variability than the maximum temperature, with significant upward trends in eight months. Minimum temperature had statistically significant trends in most months except for January, March and October. Temperature for most areas increased during the study period. Warming areas were mainly located in the northern and central NAECoS. Decreasing temperature only occurred in part of the central Georgia (Figure 7B).

Atmospheric CO_2 concentration in the study area has been increasing since the beginning of the 20th century. Atmospheric CO_2 concentrations increased by about 90 ppm in this region from 1901 to 2008. From 1901 to 1950, average CO_2 concentration only increased by 16 ppm, while it increased by about 74 ppm from 1951 to 2008.

Temporal and spatial variability of ET

[Figure 9]

Figure 9 presents the interannual variability of simulated annual ET in the NAECoS area since 1900. Average ET of NAECoS was 648.3±38.6 mm from 1901 to 2008. Significant interannual variability was found, with the maximum ET of 708 mm in 1973 and the minimum ET of 603 mm in 1904. According to the Mann-Kendall test, ET had a significant upward trend with an increasing rate of 0.23 mm/year during 1901-2008 ($p < 0.01$). The average ET to precipitation ratio was 61% in the NAECoS. This result is consistent with other studies which reported the ET to precipitation ratio is over 60% globally (Oki and Kanae, 2006).

[Table IV]

Evapotranspiration has increased significantly in five months (June, July, August, September and October) since the beginning of the 20th century (Table IV). In total, average ET has increased by about 22 mm in summer and autumn since 1901. ET variations were consistent with temperature changes since minimum and average temperature also demonstrated upward trends in summer and autumn (Table III). Although the minimum and average temperature in December and February also increased significantly, they did not lead to upward trends of ET in these two months. This result suggested that some other factors such as water availability and vegetation phenology could also significantly influence ET. Precipitation demonstrated downward trends in June, July, August, although none of them was statistically significant. The inconsistency between ET and precipitation trends might imply that water availability was not a limiting factor for ET in summer in the NAECoS.

[Figure 10]

Long-term changes of ET demonstrated significant spatial variability across the NAECoS (Figure 10). About 65% of the study area experienced increasing ET since 1901. Enhanced ET mainly occurred in the northern and central NAECoS, as well as the piedmont areas in the southern NAECoS. Decreasing ET mainly distributed in the southern NAECoS, such as Florida, central and northern Georgia and western South Carolina.

Contributions of environmental factors to ET variability

[Figure 11]

[Figure 12]

The factorial model experiments indicated that the impacts of land use change on ET varied with time (Figure 11). The land use only simulation indicated that Land use change exerted

insignificant influence on ET from 1901 to 1918, while significantly increased ET during 1919-2000. ET was increased by 13.7 mm/year on average as compared with the 'control' simulation from 1919 to 2000. Land use change impact on ET decreased gradually as a result of deforestation and urbanization after 2001. Statistical analysis indicated that land use change only accounted for 15.9% of the interannual variations of ET. However, the vast area of cropland abandonment and afforestation has resulted in an upward trend of ET over the NAECoS.

Spatial distribution ET variability from the 'land use change only' simulation provided more detailed explanations of how land use change affected ET (Figure 12A). Land conversions changed ET by more than10 mm in over 65% of the study area. Increasing ET occurred mainly in the central and southern NAECoS, such as the southeastern New York, eastern Pennsylvania, Virginia, central North Carolina, western North Carolina, and northern Georgia. In the coastal plains across North Carolina, South Carolina, and Georgia where deforestation and cropland expansion happened, ET was reduced substantially.

From 1901 to 2008, climate change increased ET in 56 years but reduced ET in the rest 54 years compared with the 'control' simulation. Climate impacts on ET varied dramatically over the study area (Figure 12B). In the northern NAECoS, ET was enhanced by 0.1-0.8 mm/year, except for the Nova Scotia area in Canada. In the eastern Pennsylvania and coastal regions across Virginia, North Carolina and South Carolina, changes in ET induced by climate factors were less than 0.1mm/year. Decreasing ET occurred in the eastern Georgia, western South Carolina, central North Carolina and western Virginia (Figure 7A).

Elevated atmospheric CO_2 levels decreased ET over the study period (Figure 12C). In the first 30 years (1901-1930), CO_2 elevation decreased ET by 0.13 mm/year, while in the last 30 years (1981-2008), CO_2 reduced ET at a rate of 2.05 mm/year. On average, CO_2 elevation

decreased ET by 0.84 mm/year over the whole study period. At spatial scale, ET increased for most areas under elevated atmospheric CO_2, while ET decreased for some areas in the northern NAECoS.

DISCUSSION

Impacts of different environmental factors on ET

Results of this study supported conclusions drawn from watershed level studies which reported that afforestation increased water loss through ET (Bosch and Hewlett, 1982; Brown *et al.*, 2005). Due to higher LAI and longer growing seasons, forest tends to have higher ET than most of other land use types (Tian *et al.*, 2010). According to DLEM 2.0 simulation, afforestation occurred over 7.5% of the study area till 2000 that resulted in 26.2 mm increase in ET compared with that of 1901. This result was in line with Bosch and Hewlett's (1982) synthesis of 94 watersheds which indicated every 10% change of forest cover in river basins could result in about 40 mm changes of water fluxes.

Compared with land use change effects, climate change has more direct effects on hydrological processes (Liu *et al.*, 2008). Climate effects on ET demonstrated significant temporal variability (Figure 11). The contribution analysis suggested that climate effects accounted for 76.3% of the interannual variability of ET. To further explore the influence of climate change on ET, correlations between climate factors (precipitation and temperature) and ET were calculated. Results showed that both precipitation ($p<0.001$) and temperature ($p=0.001$) had significant positive correlations with ET, suggesting that both precipitation and temperature could significantly change ET by affecting AET or PET. Insufficient soil water supply could be a limiting factor at high temperatures (Mohan and Arumugam, 1996). For example, the maximum

temperature during the study period appeared in 1990, but it did not result in an extremely high ET in this year, indicating that other factors such as precipitation might be a limiting factor for ET. Precipitation had more influence than temperature on ET variability in the NAECoS. The spatial pattern of ET variations from the 'climate only' simulation was similar with that of precipitation (Figure 7A and Figure 12 B). In areas that received decreasing precipitation, ET demonstrated negative response to climate change and vice versa. Increasing temperature in the northern NAECoS was consistent with enhanced ET in this region, but it did not significantly increase ET in the southern NAECoS. This result conformed to the correlation analysis of climate factors (precipitation and temperature) with ET and agreed with some studies that highlighted precipitation effects on ET in terms of long-term ET variability (Jung et al., 2010; Nagler et al., 2007). However, a large proportion of the ET variations could not be explained by precipitation and temperature alone. More variables such as interactions of different climate factors and plant responses to changing climate should also be taken into consideration in interpreting climate change impacts on ET (Mohan and Arumugam 1996).

Although rising atmospheric CO_2 concentrations were proved to have negative impacts on stomatal conductance at the leaf level, increase of plant leaf area under elevated atmospheric CO_2 levels could mitigate or even overturn the negative influence at the canopy level (Lindroth, 2012). Compared with effects of climate and land use change, impact of CO_2 on ET was negligible. This result was consistent with Kergoat et al.'s (2002) conclusion that response of ET to elevated CO_2 was not significant over large areas. One possible explanation is that CO_2 concentration increase (90 ppm) from 1901 to 2008 is much lower than most CO_2 fertilization experiments conducted to determine the effects on ET (Medlyn *et al*., 2001). Therefore, atmospheric CO_2 elevation may become an important driver for ET changes with the further

increases in CO_2 concentrations as some studies projected atmosphere CO_2 may increase to 700 ppm at the end of the ^{21}th century (Houghton *et al.*, 2001). In addition, DLEM 2.0 simulation indicated that plant ET responses to elevated CO_2 were not uniform over the study area. Specifically, ET increased in the northern NAECoS while decreased in the rest of NAECoS under elevated CO_2, suggesting that the net impacts of increased LAI and decreased stomatal conductance on ET vary among different plant functional types.

Interactions of multiple environmental factors on ET variability

Factorial model simulations in hydrological studies have suggested the importance of interpreting impacts of different driving forces on water fluxes from both temporal and spatial perspectives (Piao *et al.*, 2007; Shi *et al.*, 2011). Since CO_2 had relatively insignificant impacts on ET, here only the interactions between climate and land use change are discussed. Contribution analysis showed that climate factors and land use changes impacted ET on different temporal scales. As was discussed in the previous section, climate change was the primary driver of ET changes on the interannual scale. Unlike climate factors, land use change only accounted for 15.8% of the temporal variability of ET. However, land use changes greatly enhanced ET and induced an upward trend in ET over the whole study period. Results of this study were in line with previous studies that emphasize the significant impacts of human activities on the land surface water cycling (Schilling and Libra, 2003; Almeida *et al.*, 2007).

The spatial pattern of ET variability was determined by both land use change and climate change (Figure 10 and Figure 12). However, the two drivers contributed to the spatial pattern of ET changes at different spatial scales. To discuss the difference, we defined ‘regional scale’ as the whole study area and ‘watershed scale’ as area smaller than 10000 km^2 in this study. Climate

change played more critical in ET spatial variability than land use change at regional scale, whereas land use change significantly affected ET at watershed scales. By comparing Figure 9 with Figure 11B, the spatial distribution of ET changes were similar to the results generated from the 'climate only' simulation. Both figures showed increasing ET in most areas of the northern NAECoS and decreasing ET in some areas of the southern NAECoS. One topic that is under debate is the effects of different environmental factors on the long-term variability of water fluxes (Vorosmarty and Sahagian, 2000; Wang *et al.*, 2008). Since climate conditions have direct control on water cycling, some researchers highlighted the importance of climate change effects on ET (Pielke and Downton, 2000; Qian *et al.*, 2007). Our study results were consistent with Qian et al's (2007) which found that climate change played the dominant role in variations of water fluxes over regional scales. At watershed levels, land use change, especially afforestation, had more influence on ET than climate change. For example, climate change resulted in decreasing ET in the piedmont region (Figure 12B). However, land use dramatically increased ET in this area due to cropland abandonment and afforestation and offset the impacts from climate change (Figure 10 and Figure 12A). On the contrary, in the central NAECoS where a significant portion of the cropland was replaced by forest, both magnitudes and total areas with enhanced ET by afforestation were reduced by climate change. Therefore, results of this study indicated the importance of considering climate change and land use interactions in assessing long-term land use change influence on long-term ET variability (Jones and Post, 2004).

Implications for future water resource management and land use policy making

Understanding the mechanisms that govern ET variability is helpful for regional water resource management as ET is an important component of land surface hydrology. Drought induced by increasing ET could lead to a series of social, environmental, and economical

problems such as water scarcity and wildfire (Rind *et al.*, 1990; Zhao and Running, 2010). Contribution analysis of this study suggested that climate factors determined the spatial pattern and interannual variability of ET over the whole study area. Interaction of the changing climate factors will probably further alter the spatial patterns and the magnitude of ET and thus result in intensifying drought in some areas of the NAECoS (Mulholland *et al.*, 1997). This study also indicated afforestation in central and southern parts of NAECoS increased ET dramatically and contributed to the increasing trend of ET. Results of this study highlighted the need of considering land use change effects for water resource management at local or watershed levels. As population growth and urban expansion continues in the NAECoS, it was reported that large area of forest land disappeared because of urban sprawl in recent years (Drummond and Loveland, 2010). How these land conversions affect regional ET and other hydrological processes ought to be further investigated in the future.

Results of this study also provided valuable information for land use policy making. Since the beginning of the 20th century, large area of cropland in the NAECoS has been replaced by forest. Afforestation from agricultural land has multiple benefits for both natural ecosystem and human society such as biodiversity protection, water quality improving, and carbon sequestration (Farley *et al.*, 2005; Jackson *et al.*, 2005). However, the hydrological impacts of afforestation should not be ignored. This study has shown that in the NAECoS, 7.5% increase of forest area has increased annual ET by 12.8 mm, which means approximately 11 km^3 of freshwater was consumed by afforested areas each year. Land surface runoff is expected to decrease due to the enhanced ET, which may also affect fresh water availability for the increasing social and economic water demands in this region. In spite of the multiple benefits from afforestation, its

impacts on regional water resources should be considered in land use policy making, especially in such a densely populated region.

ACKNOWLEDGEMENTS

This study has been supported by NASA Interdisciplinary Science Program (NNX11AD47G). We thank Dr. Mingliang Liu for his efforts in model development. We also appreciate the AmeriFlux researchers and the Numerical Terra dynamic Simulation Group (NTSG) for their efforts in data collection and management.

REFERENCE

Allen, R.G., Pereira, L.S., Raes, D., Smith, M., 1998. Crop evapotranspiration: guidelines for computing crop water requirements, Rome, Italy.

Almeida CD, Vorosmarty CJ, Hurtt GC, Marengo J., Dingman SL, Keim BD. 2007. The effects of deforestation on the hydrological cycle in Amazonia : a review on scale and resolution. *International Journal of Climatology* **27**: 633–647.

Baker JT, Allen LH, Jr, Boote KJ, Jones P, Jones JW. 1990. Rice Photosynthesis and Evapotranspiration in Subambient, Ambient, and Superambient Carbon Dioxide Concentrations. *Agronomy Journal* **82**: 834–840.

Belmans C, Wesseling JG, Feddes RA. 1983. Simulation Model of the Water Balance of a Cropped Soil: SWATRE. *Journal of Hydrology* **63**: 271–286.

Bormann H, Breuer L, Gräff T, Huisman J a. 2007. Analysing the effects of soil properties changes associated with land use changes on the simulated water balance: A comparison of three hydrological catchment models for scenario analysis. *Ecological Modelling* **209**: 29–40.

Bosch JM, Hewlett JD. 1982. A review of Catchment Expreriments to Determine the Effect of Vegetation Changes on Water Yield and Evapotranspiration. *Journal of Hydrology* **55**: 3–23.

Chen G, Tian H, Zhang C, Liu M, Ren W, Zhu W, Chappelka AH, Prior S a., Lockaby GB. 2012. Drought in the Southern United States over the 20th century: variability and its impacts on terrestrial ecosystem productivity and carbon storage. *Climatic Change* **114**: 379–397.

Chen JM, Chen X, Ju W, Geng X. 2005. Distributed hydrological model for mapping evapotranspiration using remote sensing inputs. *Journal of Hydrology* **305**: 15–39.

Drummond M a., Loveland TR. 2010. Land-use Pressure and a Transition to Forest-cover Loss in the Eastern United States. *BioScience* **60**: 286–298.

Dunn SM, Mackay R. 1995. Spatial variation in evapotranspiration and the influence of land use on catchment hydrology. *Journal of Hydrology* **171**: 49–73.

Farley K a., Jobbagy EG, Jackson RB. 2005. Effects of afforestation on water yield: a global synthesis with implications for policy. *Global Change Biology* **11**: 1565–1576.

Goyal RK. 2004. Sensitivity of evapotranspiration to global warming: a case study of arid zone of Rajasthan (India). *Agricultural Water Management* **69**: 1–11.

Hijmans RJ, Cameron SE, Parra JL, Jones PG, Jarvis A. 2005. Very high resolution interpolated climate surfaces for global land areas. *International Journal of Climatology* **25**: 1965–1978.

Huntzinger DN, Post WM, Wei Y, Michalak a. M, West TO, Jacobson a. R, Baker IT, Chen JM, Davis KJ, Hayes DJ, et al. 2012. North American Carbon Program (NACP) regional interim synthesis: Terrestrial biospheric model intercomparison. *Ecological Modelling* **232**: 144–157.

Jackson RB, Jobbágy EG, Avissar R, Roy SB, Barrett DJ, Cook CW, Farley K a, le Maitre DC, McCarl B a, Murray BC. 2005. Trading water for carbon with biological carbon sequestration. *Science (New York, N.Y.)* **310**: 1944–7.

Jones J a., Post D a. 2004. Seasonal and successional streamflow response to forest cutting and regrowth in the northwest and eastern United States. *Water Resources Research* **40**: n/a–n/a.

Jung M, Reichstein M, Ciais P, Seneviratne SI, Sheffield J, Goulden ML, Bonan G, Cescatti A, Chen J, de Jeu R, et al. 2010. Recent decline in the global land evapotranspiration trend due to limited moisture supply. *Nature* **467**: 951–954.

Kergoat L, Lafont S, Douville H, Berthelot B, Dedieu G, Planton S, Royer J-F. 2002. Impact of doubled CO 2 on global-scale leaf area index and evapotranspiration: Conflicting stomatal conductance and LAI responses. *Journal of Geophysical Research* **107**: 4808.

Klein Goldewijk K, Ramankutty N. 2004. Land cover change over the last three centuries due to human activities: The availability of new global data sets. *GeoJournal* **61**: 335–344.

Latifovic R, Zhu Z, Cihlar J, Giri C, Olthof I. 2004. Land Cover Mapping of North and Central America - Global Land Cover 2000. *Remote Sensing of Environment* **891**: 116–127.

Law BE, Falge E, Gu L, Baldocchi DD, Bakwin P, Berbigier P, Davis K, Dolman AJ, Falk M, Fuentes JD, et al. 2002. Environmental controls over carbon dioxide and water vapor exchange of terrestrial vegetation. *Agricultural and Forest Meteorology* **113**: 97–120.

Lehner B, Döll P. 2004. Development and validation of a global database of lakes, reservoirs and wetlands. *Journal of Hydrology* **296**: 1–22.

Lindroth A. 1996. Will rising levels of atmospheric CO , and temperature lead to enhanced or suppressed rates of evapotranspiration ? A comment. *Weather* **51**: 285–288.

Liu M, Tian H, Chen G, Ren W, Zhang C, Liu J. 2008. Effects of Land-Use and Land-Cover Change on Evapotranspiration and Water Yield in China During 1900-2000. *JAWRA Journal of the American Water Resources Association* **44**: 1193–1207.

Liu M, Tian H, Lu C, Xu X, Chen G, Ren W. 2012. Effects of multiple environment stresses on evapotranspiration and runoff over eastern China. *Journal of Hydrology* **426-427**: 39–54.

Liu M, Tian H, Yang Q, Yang J, Song X, Lohrenz SE, Wei-jun. C. 2013. Long-term trends in evapothranspiration and runoff over the drainage basins of the Gulf of Mexico during 1901-2008. *Water Resources Research* **49**: 1988–2012.

Lu C, Tian H. 2012. Net Greenhouse Gas Balance in Response to Nitrogen Enrichment: Perspectives from a Coupled Biogeochemical Model. *Global Change Biology* **19**: 571–588.

Medlyn BE, Barton CVM, Broadmeadow MSJ, Ceulemans R, Angelis P De, Forstreuter M, Freeman M, Jackson SB, Kellomäki S, Laitat E, et al. 2001. Stomatal conductance of forest species after long-term exposure to elevated CO 2 concentration : a synthesis. *Phytologist* **149**: 247–264.

Mesinger F, DiMego G, Kalnay E, Mitchell K, Shafran PC, Ebisuzaki W, Jović D, Woollen J, Rogers E, Berbery EH, et al. 2006. North American Regional Reanalysis. *Bulletin of the American Meteorological Society* **87**: 343–360.

Mitchell TD, Jones PD. 2005. An improved method of constructing a database of monthly climate observations and associated high-resolution grids. *International Journal of Climatology* **25**: 693–712.

Monfreda C, Ramankutty N, Foley JA. 2008. Farming the planet: 2. Geographic distribution of crop areas, yields, physiological types, and net primary production in the year 2000. *Global Biogeochemical Cycles* **22**: n/a–n/a.

Mu Q, Zhao M, Running SW. 2011. Improvements to a MODIS global terrestrial evapotranspiration algorithm. *Remote Sensing of Environment* **115**: 1781–1800.

Mulholland PJ, Best GR, Coutant CC, Hornberger GM, Meyer JL, Robinson PJ, Stenberg JR, Turner RE, Vera-herrera F, Wetzel RG. 1997. Effects of Climate Change on Freshwater Ecosystems of the South-Eastern United States and the Gulf Coast of Mexico. *Hydrological Processes* **11**: 949–970.

Nagler PL, Glenn EP, Kim H, Emmerich W, Scott RL, Huxman TE, Huete a. R. 2007. Relationship between evapotranspiration and precipitation pulses in a semiarid rangeland estimated by moisture flux towers and MODIS vegetation indices. *Journal of Arid Environments* **70**: 443–462.

Piao S, Friedlingstein P, Ciais P, de Noblet-Ducoudré N, Labat D, Zaehle S. 2007. Changes in climate and land use have a larger direct impact than rising CO2 on global river runoff trends. *Proceedings of the National Academy of Sciences of the United States of America* **104**: 15242–7.

Pielke RA, Downton MW. 2000. Precipitation and Damaging Floods : Trends in the United States , 1932 – 97. *Journal of Climate* **13**: 3625–3637.

Qian T, Dai A, Trenberth KE. 2007. Hydroclimatic Trends in the Mississippi River Basin from 1948 to 2004. *Journal of Climate* **20**: 4599–4614.

Ramankutty N, Foley J a. 1999. Estimating historical changes in global land cover : Croplands from 1700 to 1992. *Global Biogeochemical Cycles* **13**: 997–1027.

Ren W, Tian H, Xu X, Liu M, Lu C, Chen G, Melillo J, Reilly J, Liu J. 2011. Spatial and temporal patterns of CO2 and CH4 fluxes in China's croplands in response to multifactor environmental changes. *Tellus B* **63**: 222–240.

Rind D, Goldberg R, Hansen J, Rosenzweig C, Ruedy R. 1990. Potential evapotranspiration and the likelihood of future drought. *Journal of Geophysical Research* **95**: 9983–10004.

Running SW, Coughlan JC. 1988. A General Model of Forest Ecosystem Processes for Regional Applications I.Hydrologic Balance, Canopy GAS Exchange and Primary Production Processes. *Ecological Modelling* **42**: 125–154.

Schilling KE, Libra RD. 2003. Increased Baseflow in Iowa Over the Second Half of the 20th Century. *Journal of the American Water Resources Association* **39**: 851–860.

Shams S, Nazemosadat SMJ, Haghighi AAK, Parsa SZ. 2012. Effect of carbon dioxide concentration and irrigation level on evapotranspiration and yield of red bean. **2**: 2012.

Shi X, Mao J, Thornton PE, Hoffman FM, Post WM. 2011. The impact of climate, CO 2 , nitrogen deposition and land use change on simulated contemporary global river flow. *Geophysical Research Letters* **38**: n/a–n/a.

Snyder RL, Song Z, Jomaa I, Moratiel R, Swelam A, Valley N, Program SA, Shapland T. 2011. Evapotranspiration Response to Climate Change. : 91–98.

Sun G, McNulty SG, Lu J, Amatya DM, Liang Y, Kolka RK. 2005. Regional annual water yield from forest lands and its response to potential deforestation across the southeastern United States. *Journal of Hydrology* **308**: 258–268.

Tao B, Tian H, Chen G, Ren W, Lu C, Alley KD, Xu X, Liu M, Pan S, Virji H. 2013. Terrestrial carbon balance in tropical Asia: Contribution from cropland expansion and land management. *Global and Planetary Change* **100**: 85–98.

Thornton PE, Rosenbloom N a. 2005. Ecosystem model spin-up: Estimating steady state conditions in a coupled terrestrial carbon and nitrogen cycle model. *Ecological Modelling* **189**: 25–48.

Tian H, Chen G, Zhang C, Melillo JM, Hall C a. S. 2009. Pattern and variation of C:N:P ratios in China's soils: a synthesis of observational data. *Biogeochemistry* **98**: 139–151.

Tian H, Chen G, Liu M, Zhang C, Sun G, Lu C, Xu X, Ren W, Pan S, Chappelka A. 2010. Model estimates of net primary productivity, evapotranspiration, and water use efficiency in the terrestrial ecosystems of the southern United States during 1895–2007. *Forest Ecology and Management* **259**: 1311–1327.

Tian H, Lu C, Chen G, Xu X, Liu M, Ren W, Tao B, Sun G, Pan S, Liu J. 2011a. Climate and land use controls over terrestrial water use efficiency in monsoon Asia. *Ecohydrology* **4**: 322–340.

Tian H, Xu X, Lu C, Liu M, Ren W, Chen G, Melillo J, Liu J. 2011b. Net exchanges of CO 2 , CH 4 , and N 2 O between China's terrestrial ecosystems and the atmosphere and their contributions to global climate warming. *Journal of Geophysical Research* **116**: G02011.

Tian H, Chen G, Zhang C, Liu M, Sun G, Chappelka A, Ren W, Xu X, Lu C, Pan S, et al. 2012a. Century-Scale Responses of Ecosystem Carbon Storage and Flux to Multiple Environmental Changes in the Southern United States. *Ecosystems* **15**: 674–694.

Tian H, Lu C, Melillo J, Ren W, Huang Y, Xu X, Liu M, Zhang C, Chen G, Pan S, et al. 2012b. Food benefit and climate warming potential of nitrogen fertilizer uses in China. *Environmental Research Letters* **7**: 044020.

Tomer MD, Schilling KE. 2009. A simple approach to distinguish land-use and climate-change effects on watershed hydrology. *Journal of Hydrology* **376**: 24–33.

Vorosmarty CJ, Sahagian D. 2000. Anthropogenic Disturbance of the Terrestrial Water Cycle. *BioScience* **50**: 753–765.

Waisanen PJ, Bliss NB. 2002. Changes in population and agricultural land in conterminous United States counties, 1790 to 1997. *Global Biogeochemical Cycles* **16**: 84–1–84–19.

Walsh J, Wuebbles D, Authors L, Hayhoe K, Kunkel K, Climatic N, Somerville R, Diego S, Stephens G, Thorne P, et al. 2013. Our Changing Climate.

Wang K, Dickinson RE, Liang S. 2008. Observational evidence on the effects of clouds and aerosols on net ecosystem exchange and evapotranspiration. *Geophysical Research Letters* **35**: L10401.

Wei Y, Liu S, Huntzinger DN, Michalak a. M, Viovy N, Post WM, Schwalm CR, Schaefer K, Jacobson a. R, Lu C, et al. 2013. The North American Carbon Program Multi-scale Synthesis and Terrestrial Model Intercomparison Project – Part 2: Environmental driver data. *Geoscientific Model Development Discussions* **6**: 5375–5422.

Wigmosta MS, Vail LW, Lettenmaier DP. 1994. A Distributed Hydrology-vegetation Model for Complex Terrain. *Water Resources Research* **30**: 1665–1679.

Zhang Y-K, Schilling KE. 2006. Increasing streamflow and baseflow in Mississippi River since the 1940s: Effect of land use change. *Journal of Hydrology* **324**: 412–422.

Zhao M, Running SW. 2010. Drought-induced reduction in global terrestrial net primary production from 2000 through 2009. *Science (New York, N.Y.)* **329**: 940–3.

Lists of tables and figures

Table I. Summary of input dataset for DLEM 2.0 Simulation

Table II. Model simulation simulations design

Table III. Long-term trends of monthly temperature and precipitation during 1901-2008. (Tmax: daily maximum temperature; Tmin: daily minimum temperature; Tavg: daily mean temperature; Ppt: precipitation; *: $p<0.05$, **$p<0.01$)

Table IV. Seasonal changes of evapotranspiration (ET) during 1901-2008 (*: $p<0.05$; **: $p<0.01$)

Figure 1. Land use types of the NAECoS in 2005

Figure 2. Framework of major biogeochemical and hydrological processes in DLEM

Figure 3. Validation of ET simulation by DLEM with AmeriFlux observations at the North Carolina loblolly pine forest site.

Figure 4 Comparison of simulated annual ET with observations across 21 AmeriFlux Sites(Atq: Atqasuk; Bo1: Bondville; Bkg: Brookings; Fpe: Fort Peck; Ha1: Harvard Forest; Ho1: Howland Forest Main; Los: Lost Creek; Me2: Metolius Intermediate Pine; Moz: Missouri Ozark; MMS: Morgan Monroe State Forest; NC2: North Carolina Loblolly Pine; NR1: Niwot Ridge; SO2: Sky Oaks Old; Syv: Tonzi Ranch; Ton: Tonzi Ranch; UMB: UMBS; Var: Vaira Ranch; WBW: Walker Branch; Wlr: Walnut River; WCr: Willow Creek).

Figure 5. Comparison of average ET simulated by (A) DLEM and (B) MODIS during 2000-2008

Figure 6. Spatial distribution of (A) cropland and (B) forest cover changes in the NAECoS from 1901 to 2008

Figure 7. Long term changes of annual precipitation and temperature over the NAECoS from 1901 to 2008 (A: precipitation: mm/year/year; B: temperature: °C /year). Mann-Kendall test was performed to check whether the changes are significant or not at the confidence level of 95% ('Increasing' suggests the upward trend, 'Decreasing' for downward trend, 'not significant' means P value for the trend is over 0.05).

Figure 8. Temporal variability of mean annual temperature and precipitation of the NAECoS during 1901-2008

Figure 9 Long-term trend of annual ET in the NAECoS during 1901-2008

Figure 10. Spatial distribution of ET variances during 1901-2008

Figure 11. Contribution analyses of climate change, land use change and atmospheric CO_2 increase on ET temporal variations. Contribution of land use change on ET was calculated by subtracting ET estimation in the 'Control' simulation from the 'Land use only' simulation (Table I). Contribution of Climate change of ET was estimated as the difference of ET between the 'Control' simulation and the 'Climate only' simulation. Contribution of CO_2 was obtained by subtracting the 'Control' simulation from the 'CO_2' only simulation. Total contribution of the three factors was calculated by subtracting ET estimation of the 'Control' simulation from the 'All' simulation.

Figure12. Variability of ET from the factorial simulations (A: 'land use only' simulation; B: 'climate only' simulation; C: 'CO_2 only' simulation)

Table I. Summary of input dataset for DLEM 2.0 Simulation

Dataset	Name	Resolution	Reference or source
Land use data	HYDE2005	0.5°×0.5°	Klein Goldewijk and Ramankutty (2004) http://gcmd.nasa.gov/index.html
	Global Lakes and Wetlands Database	Polygons for lakes over 1 km^2	Lehner and Döll (2004) http://www.wwfus.org/science/data.cfm
	Global Potential Vegetation Dataset	5×5 arc minutes	Ramankutty and Foley (1999) (http://www.sage.wisc.edu/download/potveg/global_potveg.html)
	Cropland area	0.5°×0.5°	Monfreda *et al.*(2008) http://www.geog.mcgill.ca/~nramankutty/Datasets/Datasets.html
	GLC2000	1× 1 km	Latifovic *et al.*, (2004) (http://bioval.jrc.ec.europa.eu/products/glc2000/products.php)
Irrigation data	GIAM	10× 10 km	http://www.fao.org/nr/water/aquastat/irrigationmap/index60.stm
Climate data	North America Regional Reanalysis	32×32 km	Mesinger *et al.*, (2006) http://www.emc.ncep.noaa.gov/mmb/rreanl/
	CRU Global Climate Dataset	0.5°×0.5°	Mitchell and Jones (2005) http://www.ipcc-data.org/obs/cru_climatologies.html
Atmospheric CO_2 data	Global CO_2 concentration data	0.5°×0.5°	Wei *et al.*, (2013)

Table II. Model simulation simulations design

Name	Changing environmental factors	Objective
Control	No environmental changes since 1901	Provide a baseline for the other simulations
Climate only	Climate change(precipitation and temperature)	Assess the climate change effect on ET.
Land use only	Land cover change and related management activities such as irrigation and fertilization	Assess the land use change effect on ET.
CO_2 only	Atmosphere CO_2 concentration	Assess the impacts of enhanced CO_2 on ET
All	Land use change, increasing atmospheric CO_2, and changing climate conditions	Total effects environmental changes on ET

Table III. Long-term trends of monthly temperature and precipitation during 1901-2008 (Tmax: daily maximum temperature; Tmin: daily minimum temperature; Tavg: daily mean temperature; Ppt: precipitation; *: p<0.05, **p<0.01)

Month	**Tmax**		**Tmin**		**Tavg**		**Ppt**	
	slope	p-value	slope	p-value	slope	p-value	slope	p-value
Jan.	-0.0070	0.3156	0.0028	0.6962	0.0018	0.8000	0.0003	0.9047
Feb.	0.0137	0.0241*	0.0189	0.0017**	0.0166	0.0050**	-0.0023	0.3167
Mar.	0.0063	0.2875	0.0058	0.2624	0.0063	0.2400	-0.0003	0.9064
Apr.	0.0135	0.0008**	0.0102	0.0006**	0.0122	0.0003**	-0.0001	0.9635
May.	0.0039	0.3443	0.0072	0.0232*	0.0059	0.0857	0.0012	0.5858
Jun.	0.0039	0.1726	0.0144	0.0000**	0.0095	0.0002**	-0.0024	0.2742
Jul.	0.0020	0.4142	0.0126	0.0000**	0.0077	0.0004**	-0.0028	0.1407
Aug.	0.0059	0.0295*	0.0148	0.0000**	0.0108	0.0001**	-0.0044	0.0558
Sep.	-0.0051	0.1275	0.0079	0.0103*	0.0018	0.5319	0.0003	0.9103
Oct.	-0.0052	0.2067	0.0043	0.2860	0.00004	0.9921	0.0007	0.7959
Nov.	0.0069	0.1298	0.0185	0.0000**	0.0129	0.0017**	0.007	0.0065**
Dec.	0.0097	0.1060	0.0143	0.0094**	0.0132	0.0297*	-0.0016	0.5237

Table IV. Seasonal changes of evapotranspiration (ET) during 1901-2008 (*: p<0.05; **: p<0.01)

Month	**ET**	
	slope	**p-value**
Jan.	0.0002	**0.6821**
Feb.	-0.0078	**0.1942**
Mar.	-0.0074	**0.3111**
Apr.	0.0047	**0.6137**
May.	0.018	**0.0554**
Jun.	0.037	**0. 011***
Jul.	0.051	**<0.001****
Aug.	0.056	**<0.001****
Sep.	0.048	**<0.001****
Oct.	0.029	**0.022***
Nov.	0.0016	**0.8712**
Dec.	0.014	**0.1990**

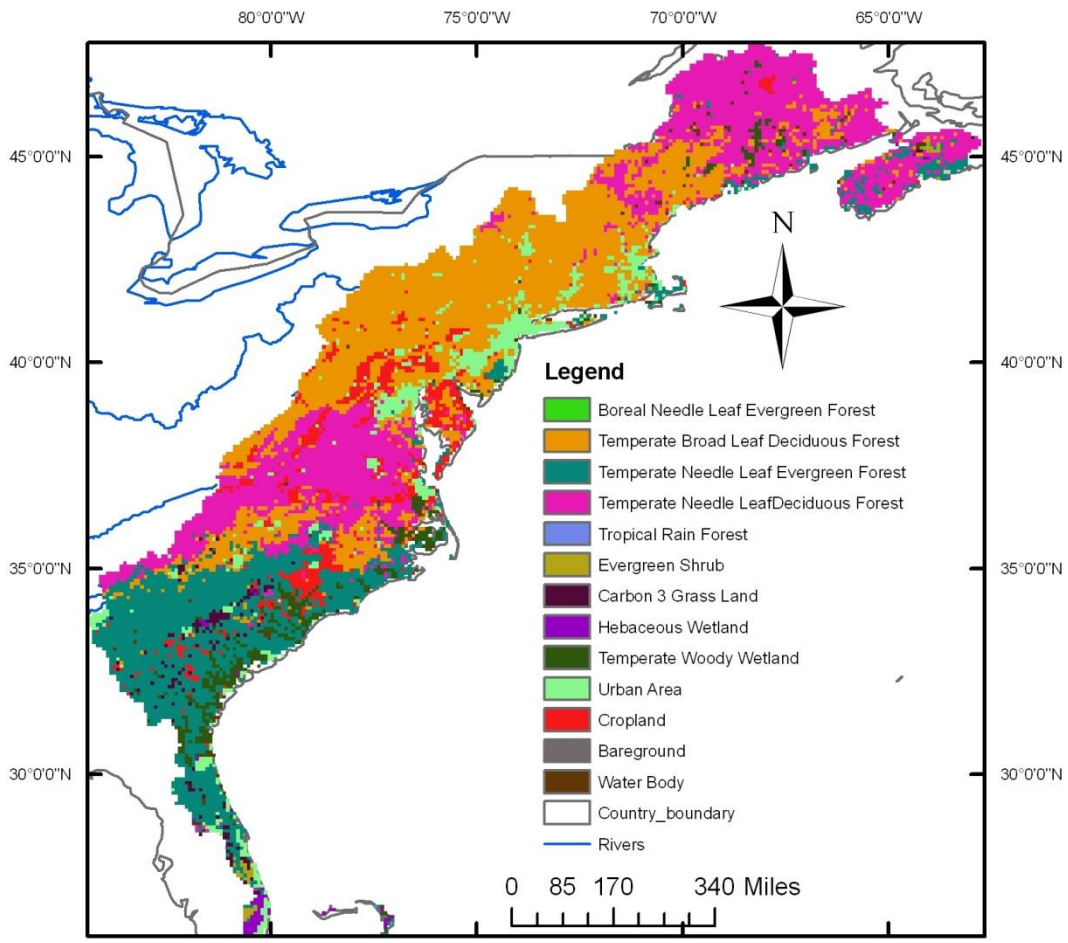

Figure 1. Land use types of the NAECoS in 2005

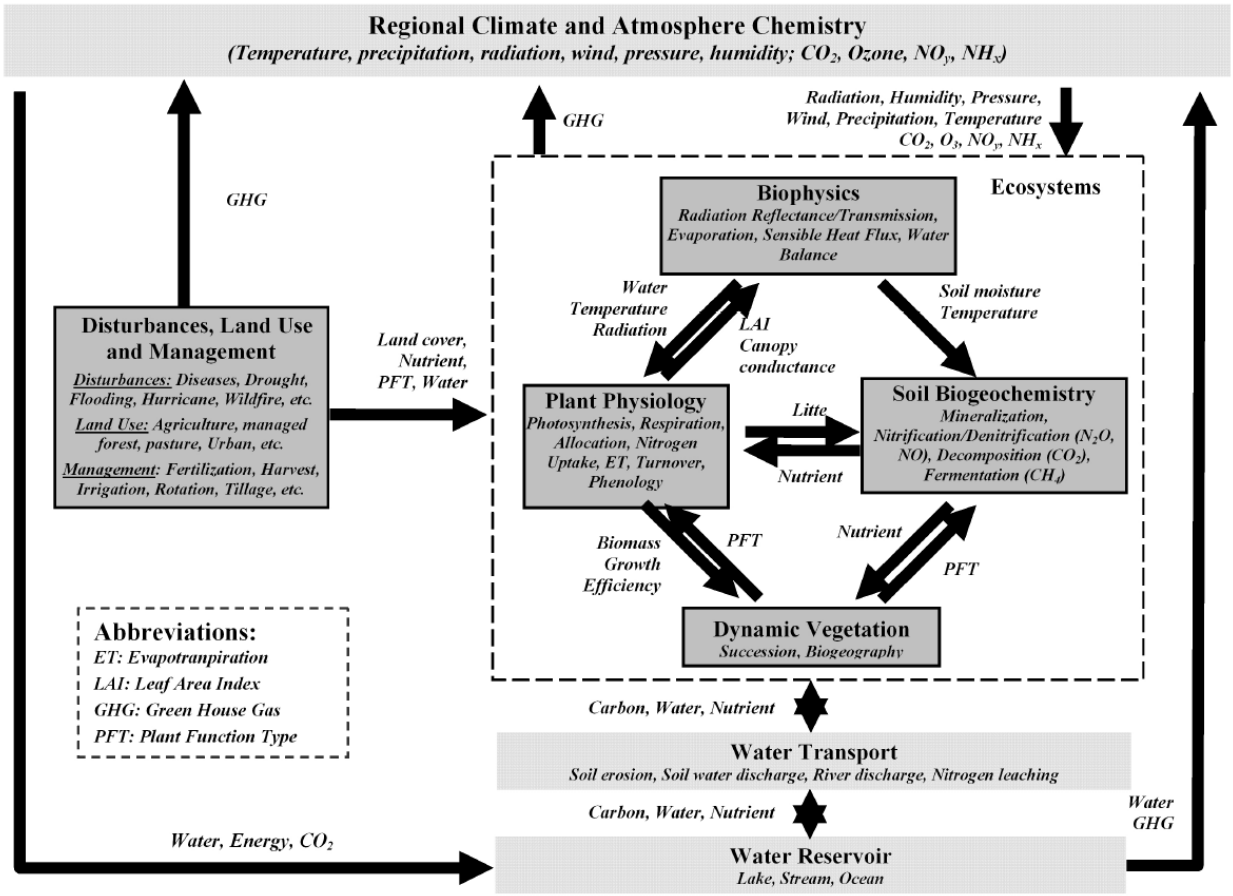

Figure 2. Framework of major biogeochemical and hydrological processes in DLEM

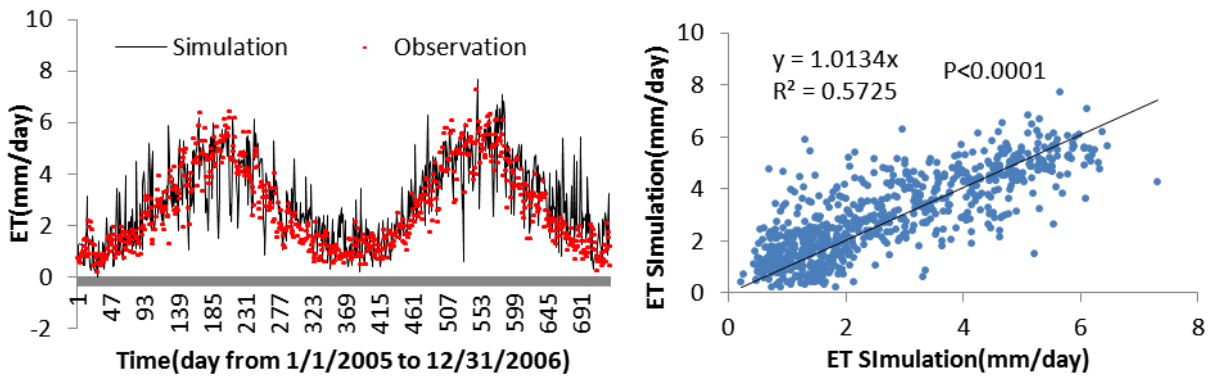

Figure 3. Validation of ET simulation by DLEM with AmeriFlux observations at the North Carolina loblolly pine forest site.

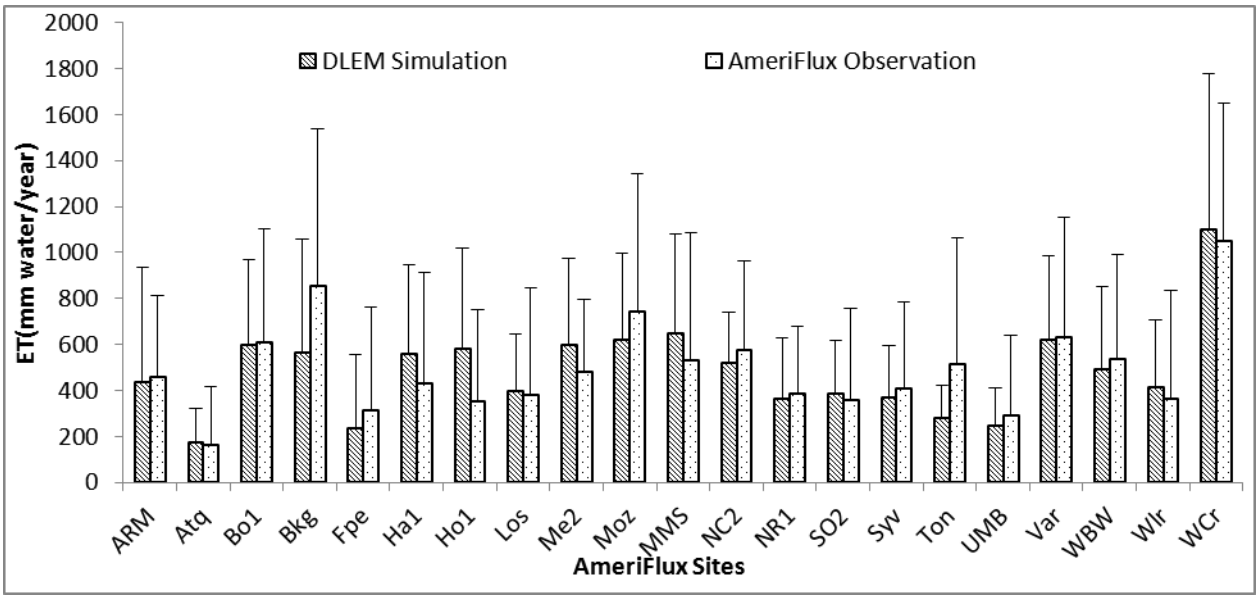

Figure 4 Comparison of average annual ET and standard deviation between DLEM simulation and observations across 21 AmeriFlux Sites. (Atq: Atqasuk; Bo1: Bondville; Bkg: Brookings; Fpe: Fort Peck; Ha1: Harvard Forest; Ho1: Howland Forest Main; Los: Lost Creek; Me2: Metolius Intermediate Pine; Moz: Missouri Ozark; MMS: Morgan Monroe State Forest; NC2: North Carolina Loblolly Pine; NR1: Niwot Ridge; SO2: Sky Oaks Old; Syv: Tonzi Ranch; Ton: Tonzi Ranch; UMB: UMBS; Var: Vaira Ranch; WBW: Walker Branch; Wlr: Walnut River; WCr: Willow Creek).

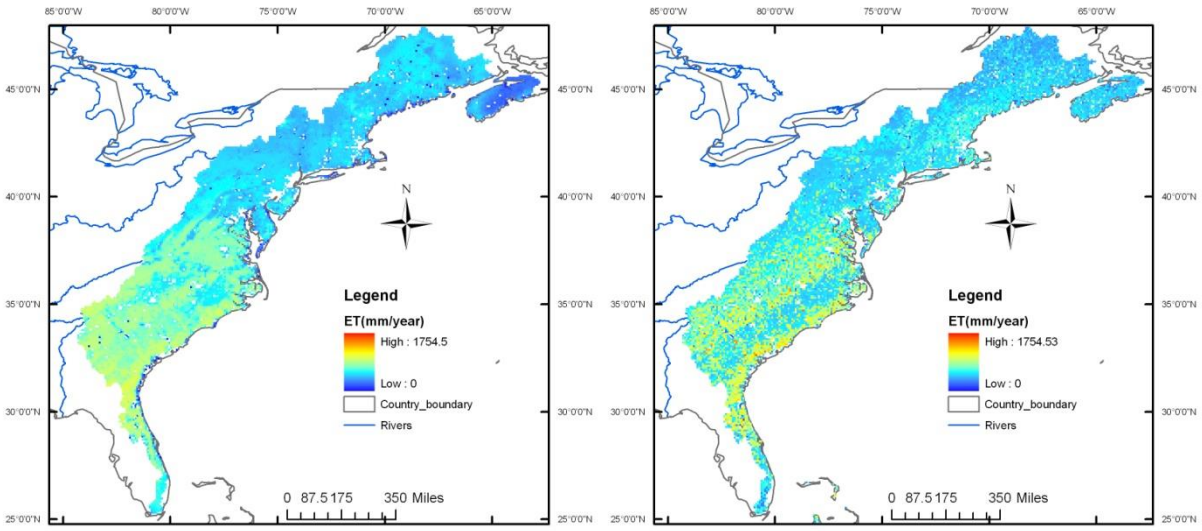

A B

Figure 5. Comparison of average ET simulated by (A) DLEM and (B) MODIS during 2000-2008

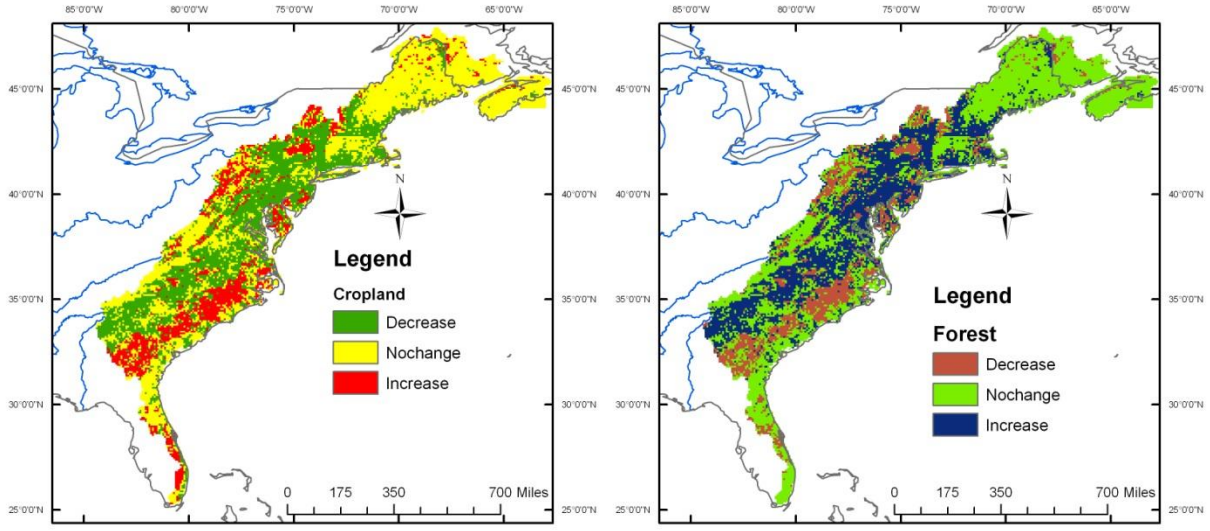

A B

Figure 6. Spatial distribution of (A) cropland and (B) forest cover changes in the NAECoS from 1901 to 2008

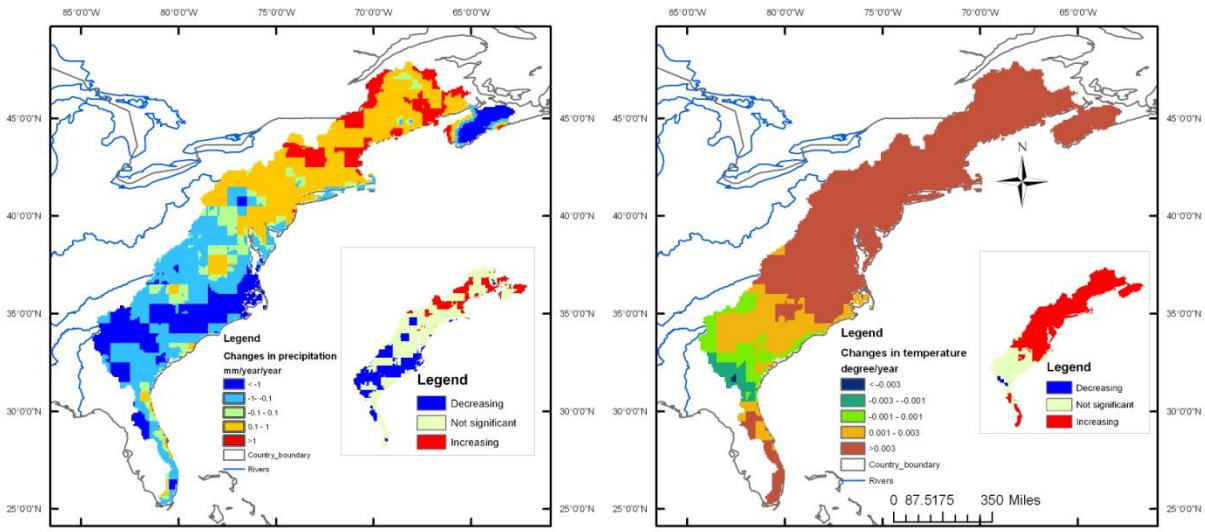

A B

Figure 7. Long term changes of annual precipitation and temperature over the NAECoS from 1901 to 2008(A: precipitation: mm/year/year; B: temperature: °C /year). Mann-Kendall test was performed to check whether the changes are significant or not at the confidence level of 95% (‘Increasing’ suggests the upward trend, ‘Decreasing’ for downward trend, ‘not significant’ means P value for the trend is over 0.05. This method was also used in Figure 10 and 12).

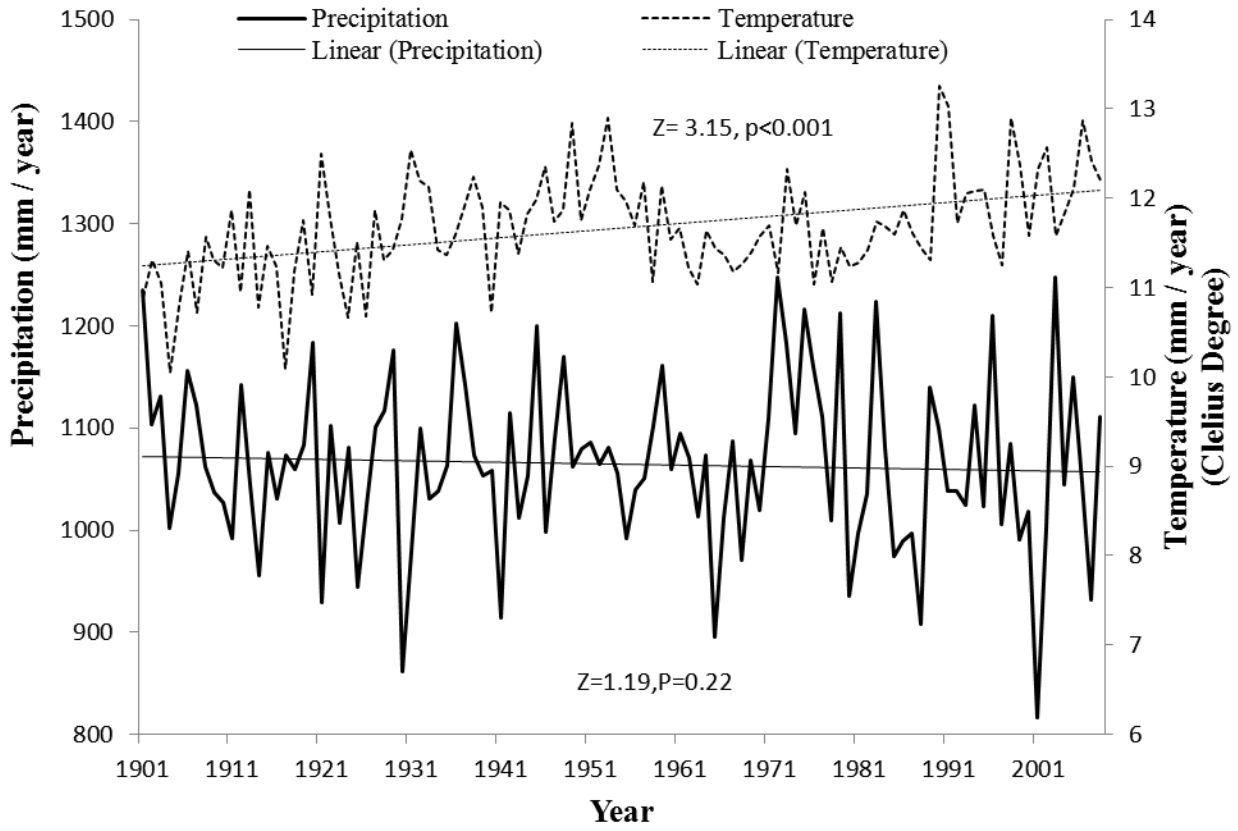

Figure 8. Temporal variability of mean annual temperature and precipitation of the NAECoS during 1901-2008

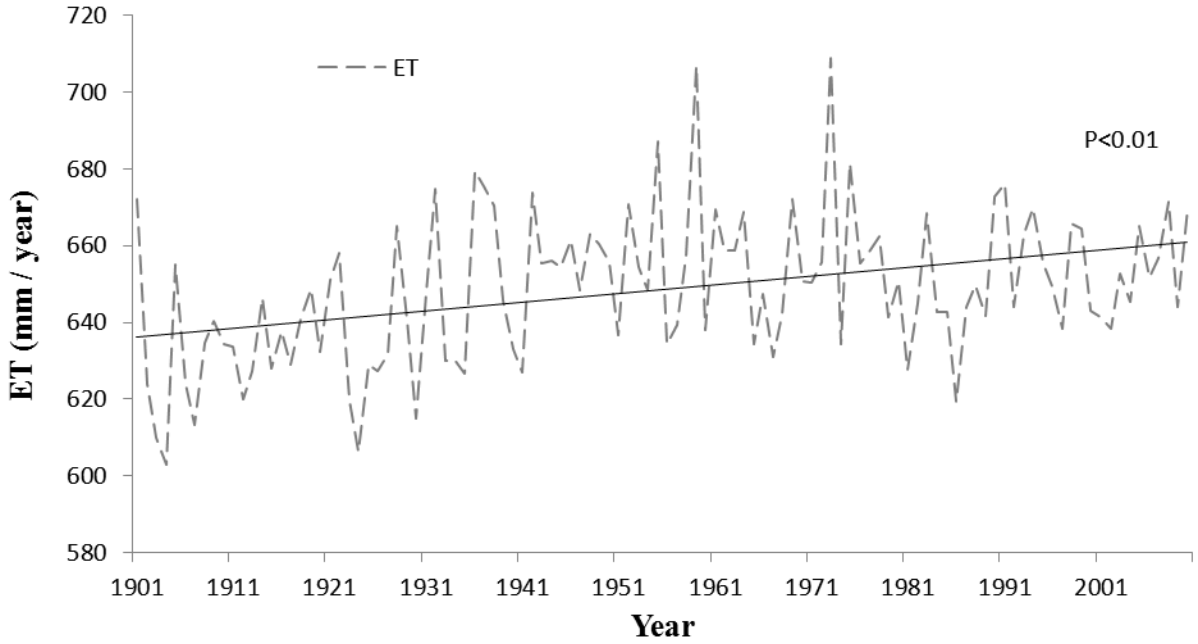

Figure 9 Long-term trend of annual ET in the NAECoS during 1901-2008

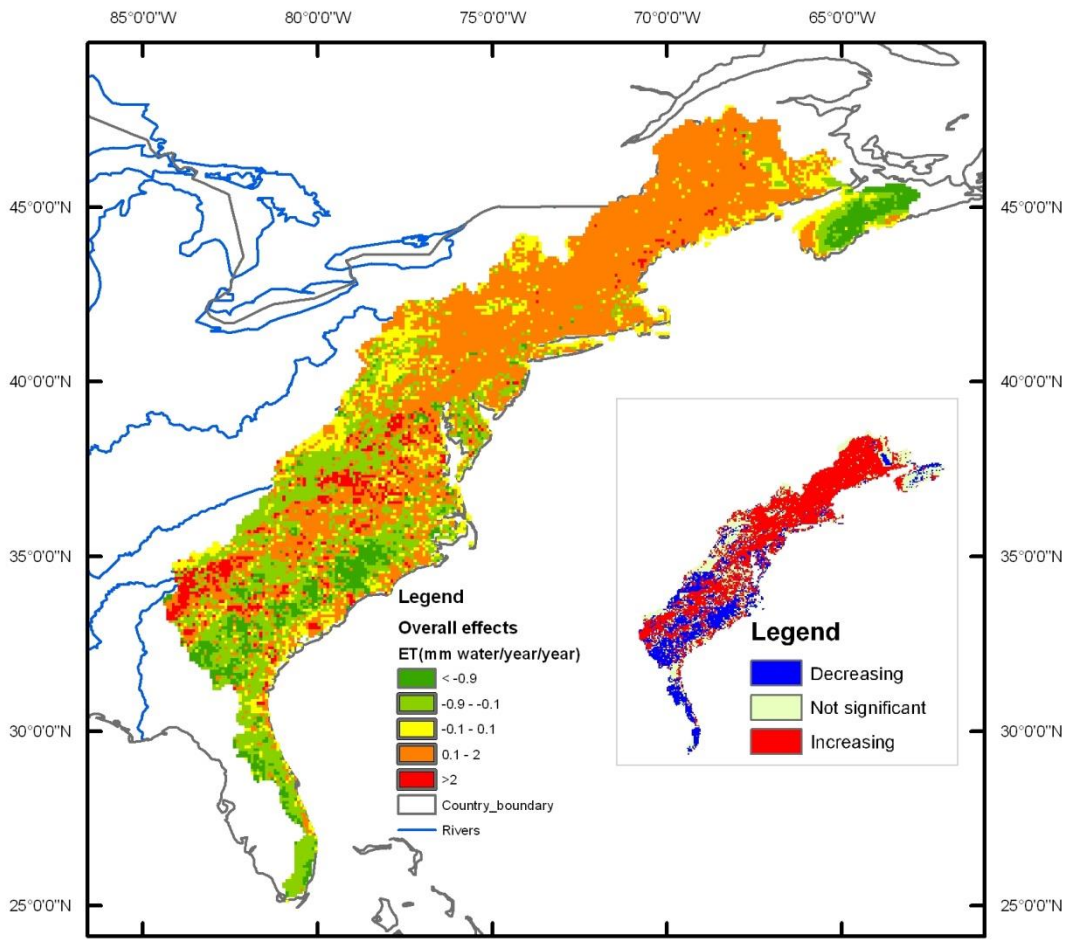

Figure 10 Spatial distribution of ET variability during 1901-2008

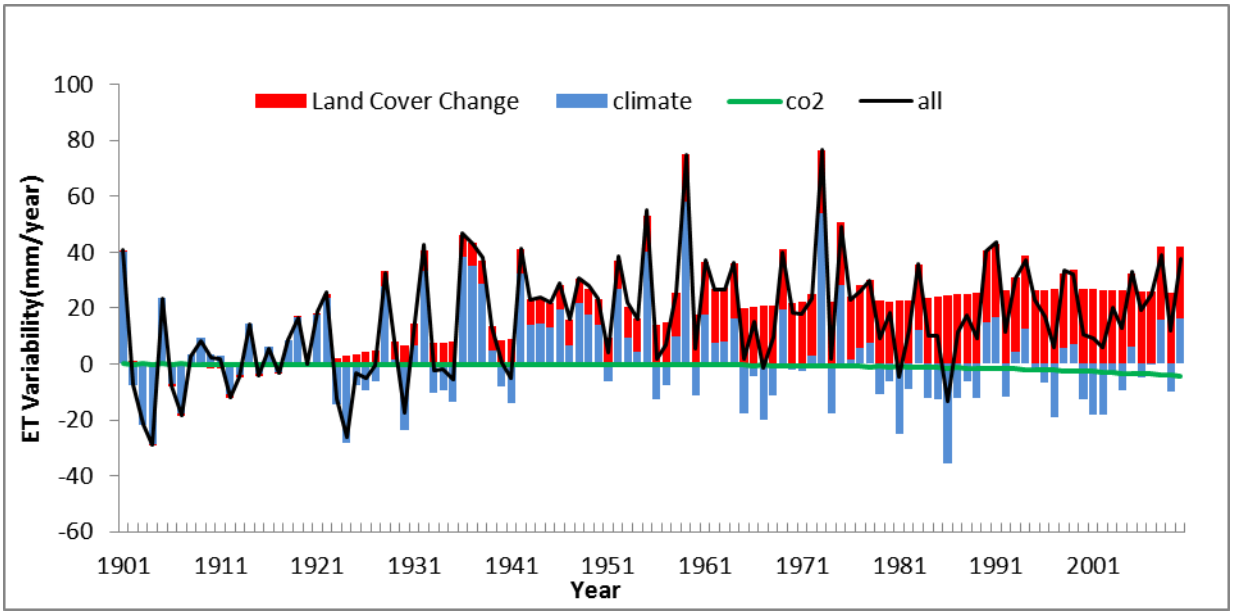

Figure 11. Contribution analyses of climate change, land use change and atmospheric CO_2 increase on ET temporal variations. Contribution of land use change on ET was calculated by subtracting ET estimation in the 'Control' simulation from the 'Land use only' simulation (Table I). Contribution of Climate change of ET was estimated as the difference of ET between the 'Control' simulation and the 'Climate only' simulation. Contribution of CO_2 was obtained by subtracting the 'Control' simulation from the 'CO_2' only simulation. Total contribution of the three factors was calculated by subtracting ET estimation of the 'Control' simulation from the 'All' simulation.

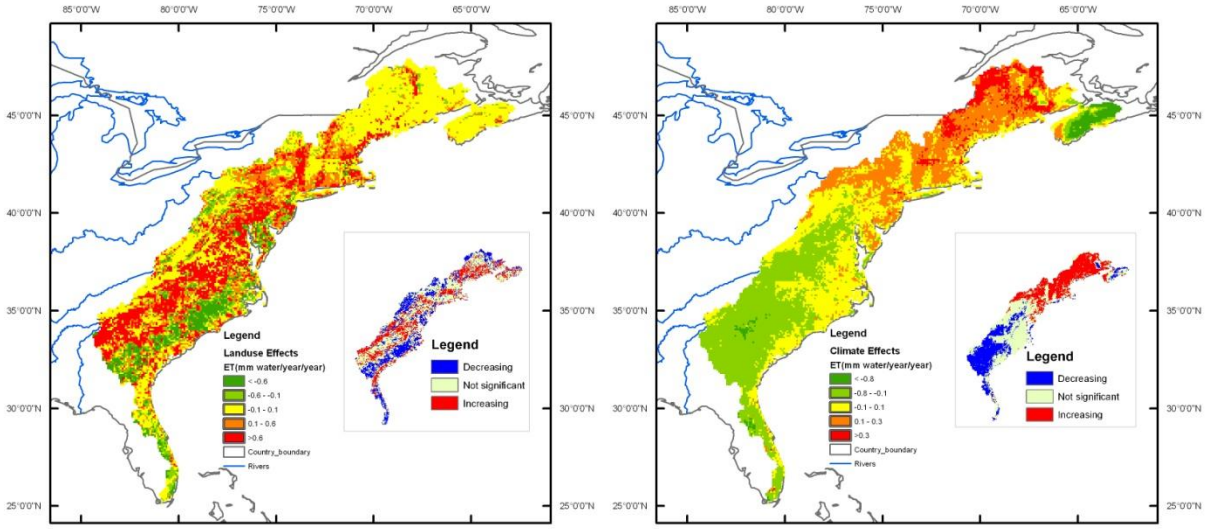

A B

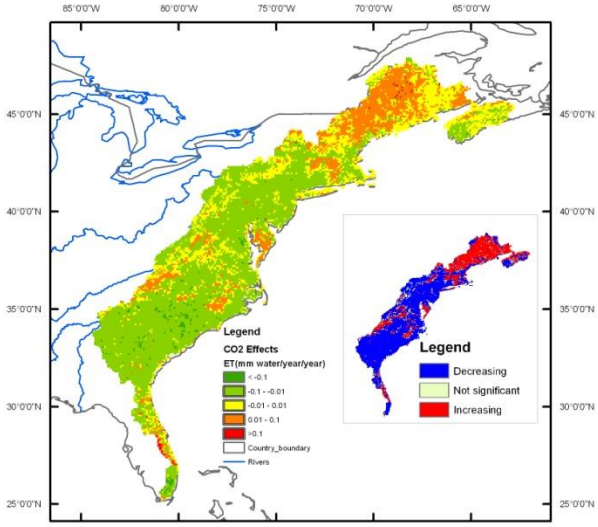

C

Figure12. Variability of ET from the factorial simulations (A: ‘land use only’ simulation; B: ‘climate only’ simulation; C: ‘CO_2 only’ simulation)